Anti-noise wave-equation traveltime inversion and application to salt estimation

Xukai Shen

ABSTRACT

The convergence of full-waveform inversion relies heavily on a good starting model. Such a model can be provided by wave-equation traveltime inversion. However, results from wave-equation traveltime inversion are susceptible to data noise, which is particularly obvious in real data applications. I propose to address this problem by replacing the real data term in back-propagation kernel with a synthetic data term that honors the traveltime information. This modification makes the inversion immune to noise in recorded data waveforms, yet results in a model that is still good for subsequent full-waveform inversion. I demonstrate this with an example of salt estimation. Salt estimation by direct full-waveform inversion is challenging due to a combination of inadequate starting models and insufficient low-frequency data. Reflection wave-equation traveltime inversion with my modification provides a good starting model for subsequent full-waveform inversion of salt estimation, even with data that lack low-frequency components.

INTRODUCTION

Data-domain tomographic methods update velocity using mismatches between observed data and modeled data. The mismatches usually include traveltime (first-order) and waveform (second-order) differences. Both traveltime and waveform mismatches are used by Full Waveform Inversion (FWI) (Tarantola, 1984; Pratt et al., 1998; Mora, 1987), leading to high-resolution results but requiring an accurate starting model. On the other hand, Wave-equation Traveltime Inversion (WTI) (Luo and Schuster, 1991) estimates velocity model by minimizing only the traveltime difference between observed data and modeled data using the wave equation. As a result, WTI differs from FWI in two ways: first, WTI is not affected by cycle skipping, and second, WTI results tend to have low resolution. However, the low-resolution result from WTI may be a good starting model, and subsequent application of FWI can obtain a high-resolution result (Shen et al., 2012).

In WTI, the back-propagation term depends linearly on the traveltime differences and time-shifted observed data. The traveltime difference in the back-propagation term makes WTI insensitive to cycle-skipping. The time-shifted observed data, on the other hand, will compromised the inversion results if observed data is contaminated with strong noise. This is likely to be true for field data, especially data acquired on land. To avoid the noise problem in field data, I propose to replace the inverse problem with a series of synthetic problems whose data traveltimes are the same as those of the original problem. When we solve the new synthetic problems, we no longer suffer from potential noise in field data, but we still obtain a similar result, since the new problems have the same data traveltimes as the original problem.

The effectiveness of the new method is demonstrated with an salt estimation example. Salt estimation with FWI is difficult. Synthetic tests suggest that even with a intuitively close starting model, very low-frequency data is required for successful inversion (Koo et al., 2009; Vigh and Starr, 2008). To lessen the requirement for low-frequency data, WTI is a good candidate. However, past success with WTI mostly has used diving waves or direct arrival (Sirgue et al., 2009; Virieux and Operto, 2009), with very few reflection cases (Zhang et al., 2011). I will demonstrate that reflection data WTI with the aforementioned modification can indeed provide a good starting model for subsequent FWI.

ANTI-NOISE WAVE-EQUATION TRAVELTIME INVERSION

The original WTI method minimizes the following objective function:

$$f(\mathbf{m}) = \sum_{s,r} \Delta\tau^2(\mathbf{m}), \tag{1}$$

where $\mathbf{m}$ is the velocity or slowness model to be estimated, s and r are source and receiver locations, respectively, and $\Delta\tau$ is defined as the time lag that maximizes the cross-correlation between the observed trace and the modeled trace. By this definition, $\Delta\tau$ is also the traveltime difference between corresponding events in synthetic data and recorded data. From this objective function, the back-propagation term for gradient calculation is

$$v_{src}(t) = \Delta\tau \frac{\dot{d_{obs}}(t+\Delta\tau)}{\dot{d_{obs}}(t+\Delta\tau) * \dot{d_{syn}}(t)}, \tag{2}$$

where $\dot{d_{obs}}$ and $\dot{d_{syn}}$ denote first-order time derivatives of observed and synthetic data, respectively. $*$ denotes cross-correlation. It can be seen that this back-propagation term is proportional to the noise strength in the observed data. To avoid potential noise effects, I will solve an equivalent synthetic problem. Notice that only the traveltime difference is used in the objective function, I can assume that the only difference between the observed data and the modeled data is the static time-shift $\Delta\tau$. This assumption is mathematically expressed as

$$d_{obs}(t+\Delta\tau) \approx d_{syn}(t). \tag{3}$$

Substituting this into equation 2, we get the new back-propagation term

$$v_{src}(t) = \Delta\tau \frac{\dot{d_{syn}}(t)}{\dot{d_{syn}}(t) * \dot{d_{syn}}(t)}. \tag{4}$$

The new back propagation term still honors the traveltime difference, yet it is completely noise-free. In other words, we use only the traveltime information from the observed data to perform the inversion. Physically, this modification means we are solving an equivalent synthetic problem at each iteration, where the new observed data is defined by equation 3. This modification completely removes the noise interference from the actual data.

SALT ESTIMATION

With the proliferation of sub-salt reservoir discoveries in recent years, sub-salt imaging has become increasingly important. It has been shown (Shoshitalshvill et al., 2006) that better definition of the salt improves sub-salt imaging. In this section, I will show how the modified WTI can help improve salt estimation by supplying FWI with a better starting model.

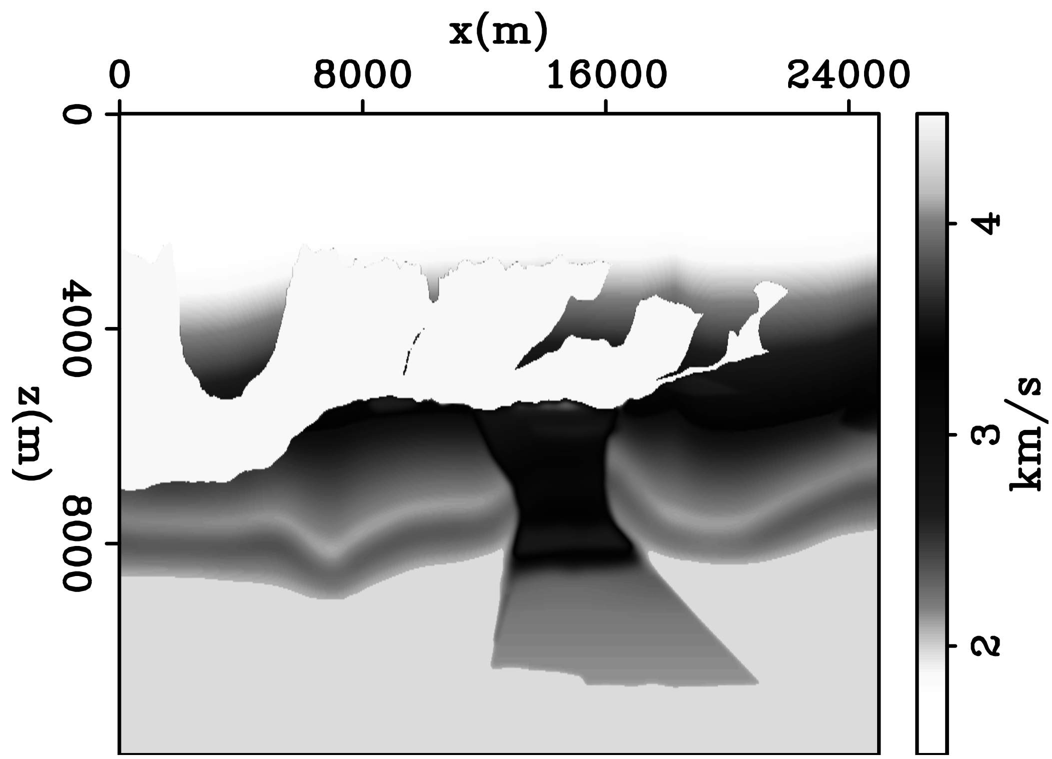

Figure 1: True velocity model for inversion. [**ER**]

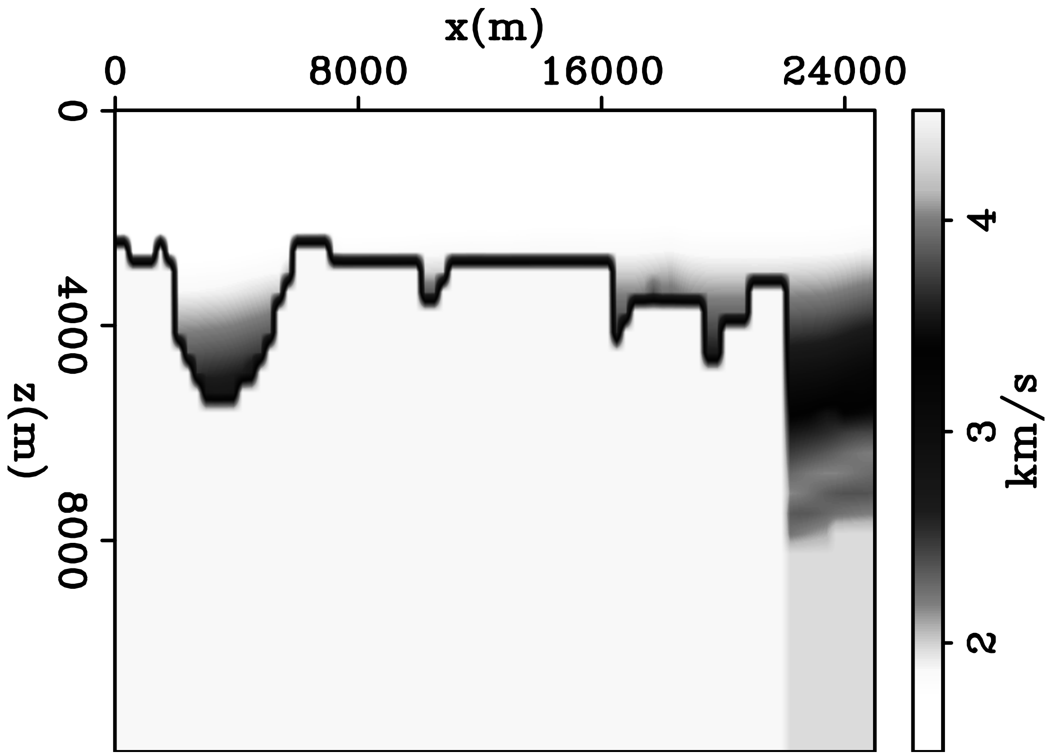

Figure 2: Starting velocity model for inversion. [**ER**]

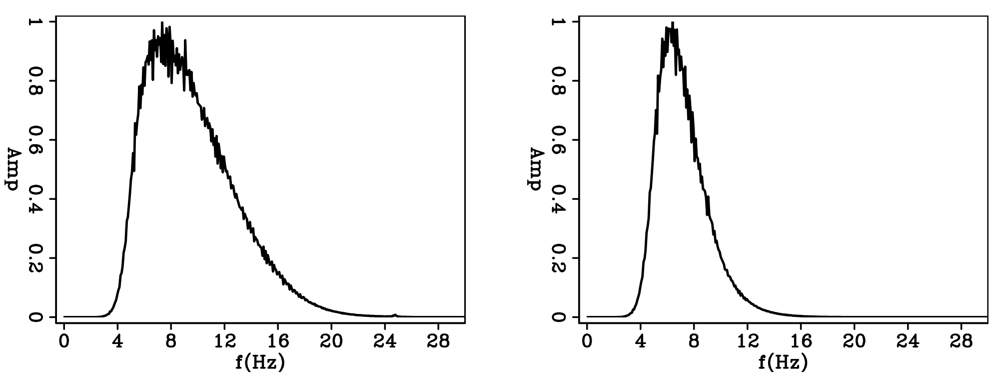

Figure 3: Spectrum of data used for a) traveltime inversion b) waveform inversion. [**ER**]

The salt model in figure 1 is taken from part of the BP 2004 Velocity Benchmark, where the top of salt formation is rugose. I modeled a total of 96 shots with constant-density acoustic modeling. Shot spacing was 250 meters. The offset range of each shot gather was from −8 km to 8 km. Both modeling and inversion were performed on a 25 m grid spacing. All inversion data lack low-frequency components (Figure 3). Only salt-related reflections are used in the inversion, with refractions, direct arrivals, and water-bottom reflections muted (Figures 4 and 5) . The starting model (figure 2) has an accurate water-bottom definition and a close-to-accurate sediment velocity down to the salt top; however, the salt top is a smoothed version of a coarse set of top-of-salt picks. Such a starting model is similar to a real data scenario, since the water bottom is usually well constrained, along with the sediment velocities down to the top of salt. Two types of inversions were performed, one performing FWI from the starting model and the other applying WTI followed by FWI.

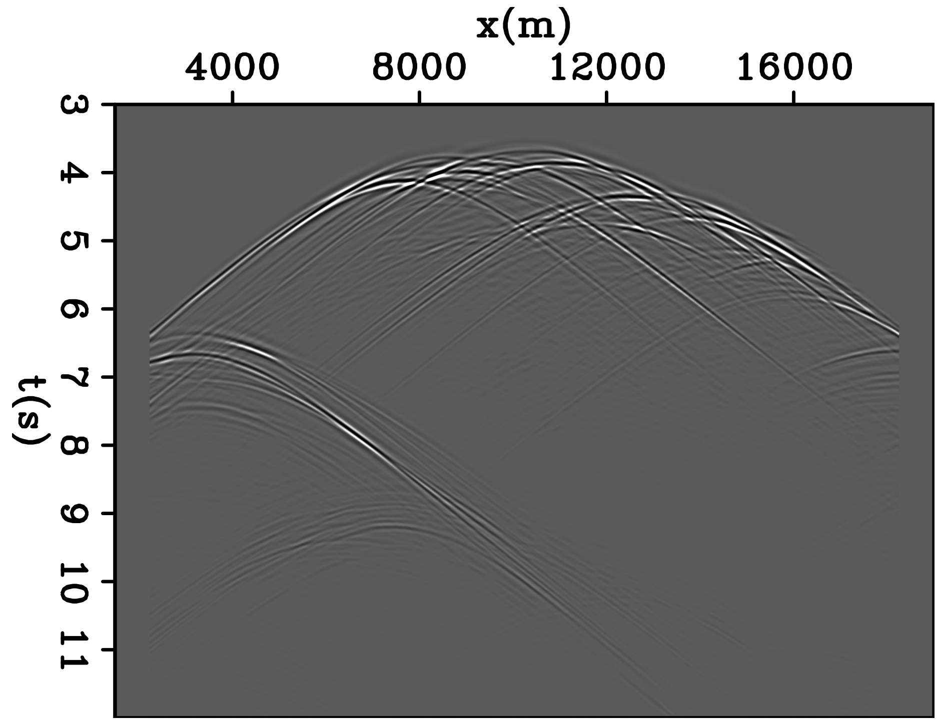

Figure 4: One shot record from the true model for WTI (reflection only). [**CR**]

Due to the inaccurate positioning of the salt top in the starting model, cycle-skipping of the salt-top reflection exists between the shot gathers modeled from the true model and the ones from the starting model (Figures 4 and 6). As a result, FWI from the starting model can not accurately put the modeled reflection at the correct traveltimes (Figures 5 and 8). On the other hand, WTI does model reflections to reasonably accurate traveltimes (Figures 4 and 7), enabling subsequent FWI to further match the detailed waveforms of observed reflections (Figures 5 and 9).

The result of FWI from the starting model is shown in figure 10, the result of WTI from the starting model is shown in figure 11, and the result of FWI after WTI

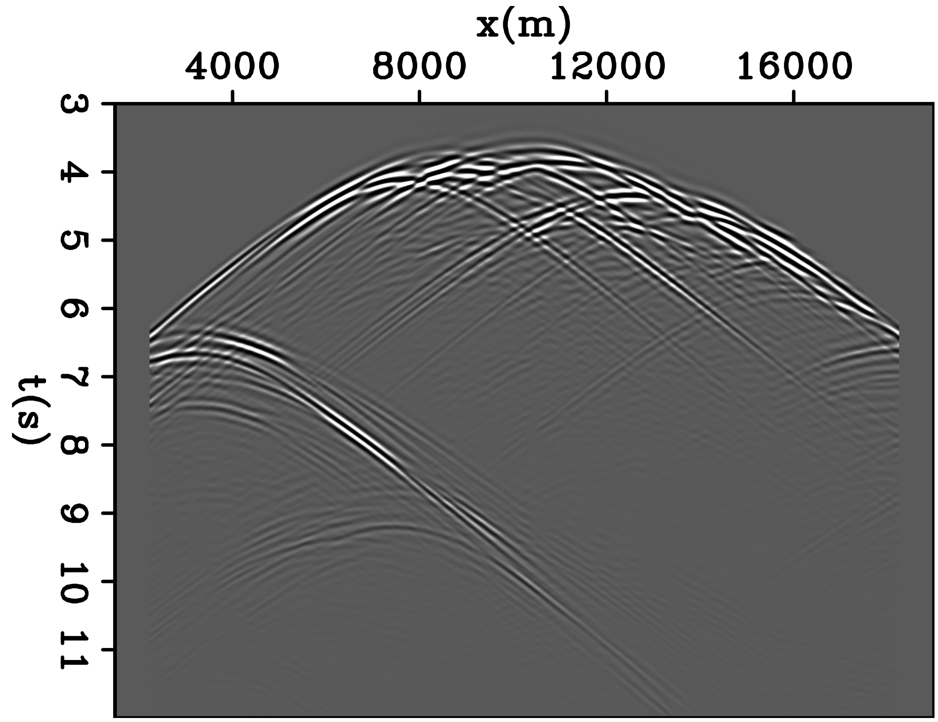

Figure 5: One shot reflection from the true model for FWI (reflection only). [**CR**]

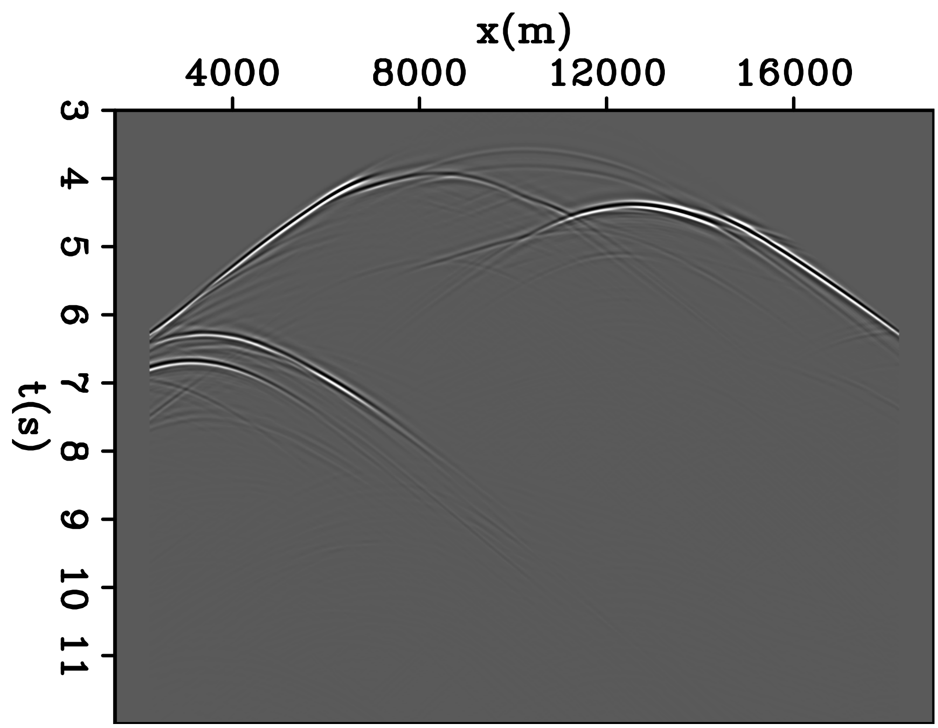

Figure 6: One shot record from the initial model (reflection only). [**CR**]

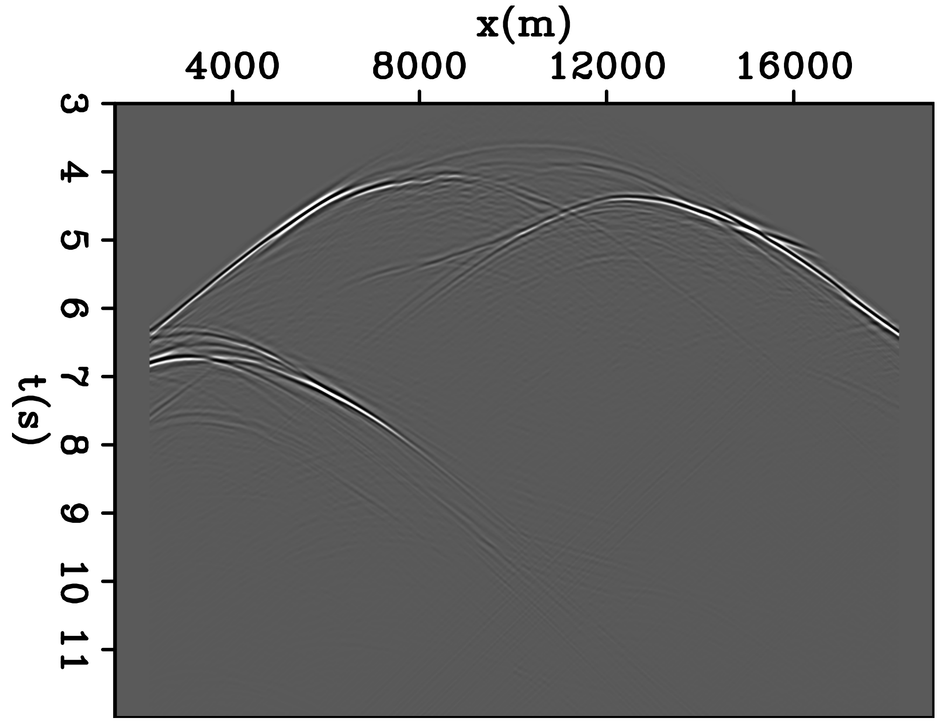

Figure 7: One shot record from the WTI result (reflection only). [**CR**]

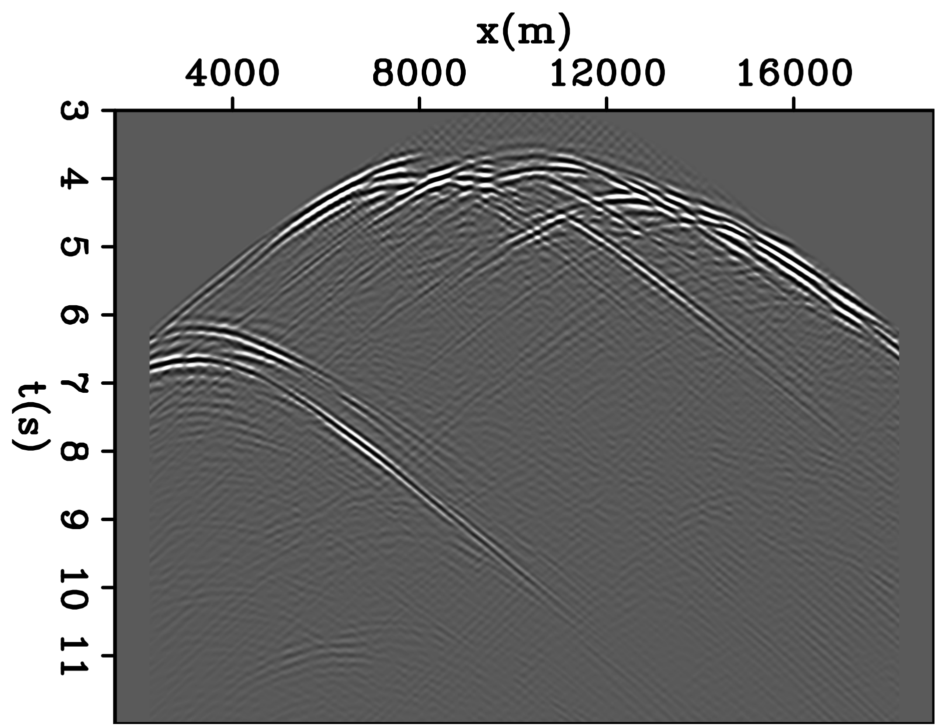

Figure 8: One shot record reflection from the direct FWI result (reflection only). [**CR**]

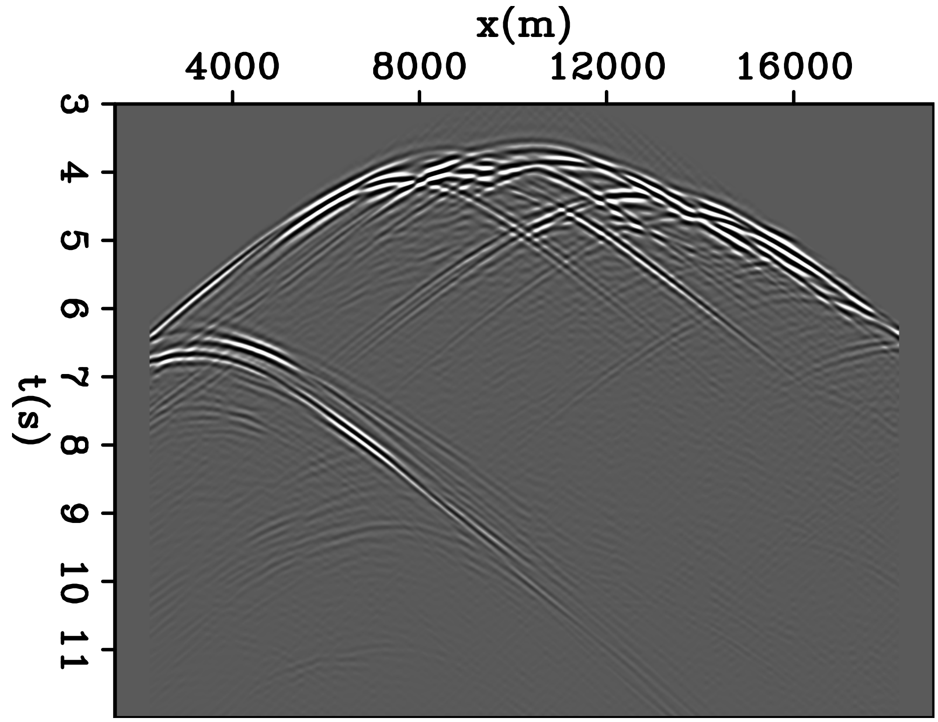

Figure 9: One shot record from the FWI (after WTI) result (reflection only). [**CR**]

is shown in figure 12. It can be seen that direct FWI neither converged to the true model nor gave a good indication of where the salt boundaries are; to make matters worse, it even produced spurious salt inclusions near the top of salt. However, WTI was able to correct the location of the salt top so that subsequent FWI accurately estimated the salt top with very high resolution. In addition, the result of FWI after WTI also yielded a good indication of the location of salt inclusions, salt flanks and the salt bottom, all of which are important information for salt-geometry estimation and sub-salt imaging.

CONCLUSION

I devised a modification to the existing WTI method to make it immune to noise in recorded data. The modification substitutes the original problem with a series of synthetic problems where mismatched traveltime is honored. Using reflection data only, application of this modified WTI followed by FWI was able to give high-resolution results of the salt top and a good indication of salt flank and bottom locations, whereas direct FWI from the starting model failed to do so.

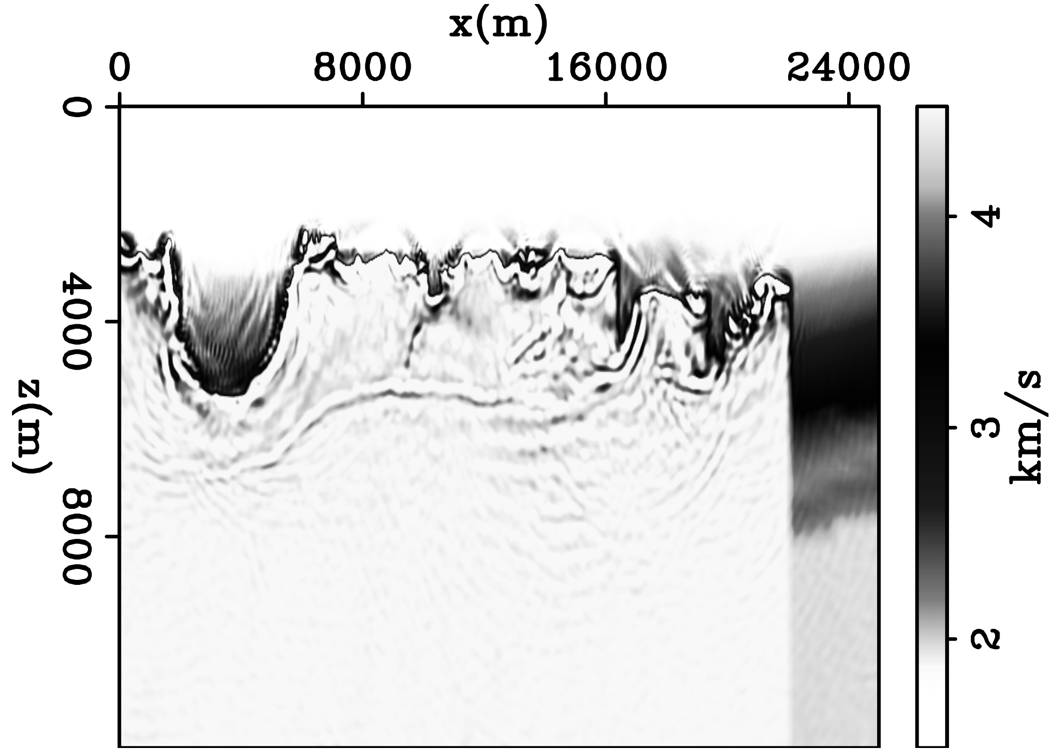

Figure 10: Result from FWI using the starting model. [**CR**]

ACKNOWLEDGMENTS

I would like to thank Dr. Luo from Saudi Aramco for suggestions/discussions on this topic.

REFERENCES

Koo, N., C. Shin, and Y. H. Cha, 2009, Sequentially ordered single-frequency 2-D acoustic waveform inversion in the Laplace-Fourier domain: SEG Technical Program Expanded Abstracts.

Luo, Y. and G. T. Schuster, 1991, Wave-equation traveltime inversion: Geophysics, **56**, 645–653.

Mora, P., 1987, Elastic wavefield inversion: SEP Ph.D Thesis.

Pratt, R. G., C. Shin, and G. Hicks, 1998, Gauss-Newton and full Newton methods in frequency domain seismic waveform inversion: Geophysical Journal International, **133**, 341–362.

Shen, X., T. Tonellot, Y. Luo, T. Keho, and R. Ley, 2012, A new waveform inversion workflow: Application to near-surface velocity estimation in Saudi Arabia: SEG Technical Program Expanded Abstracts.

Shoshitalshvill, E., S. Michell, J. Etgen, D. Chergotis, and E. Olson, 2006, Improving

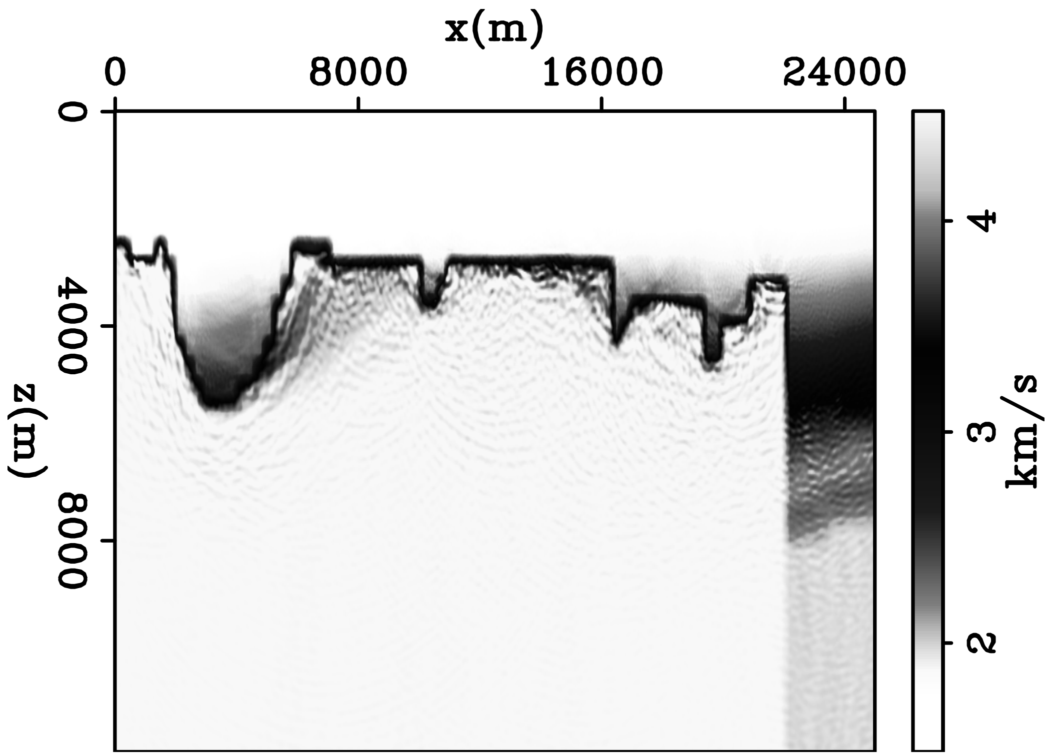

Figure 11: Result from WTI using the starting model. [**CR**]

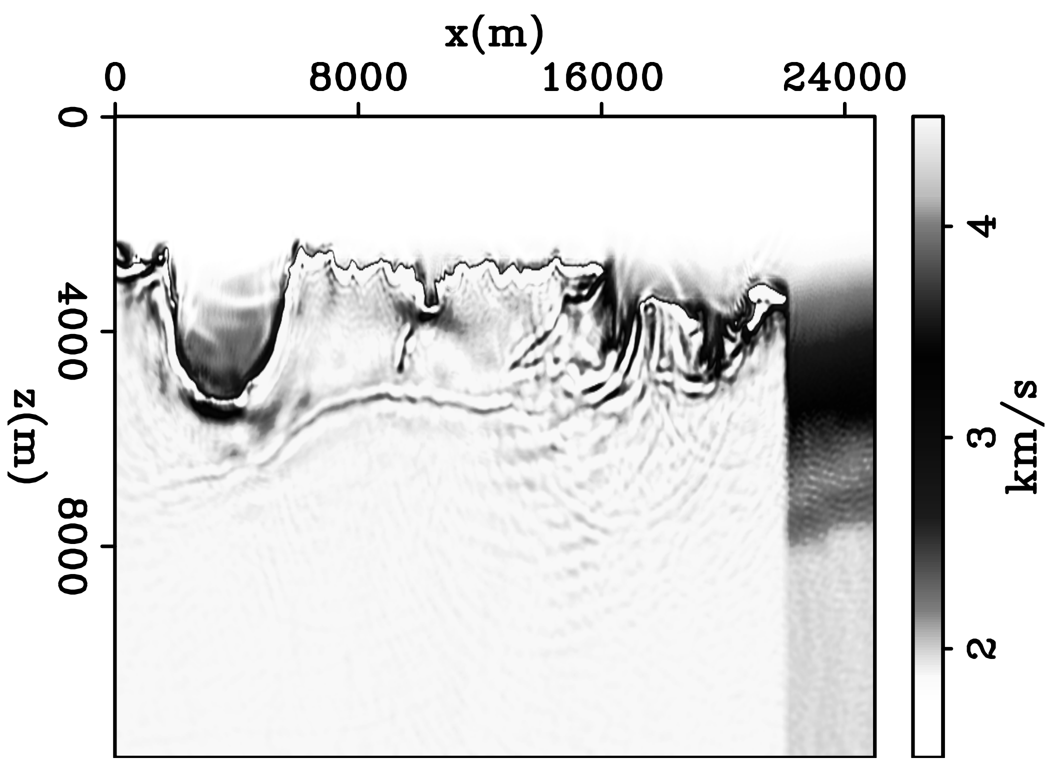

Figure 12: Result from FWI using the WTI inverted model. [**CR**]

resolution of top salt complexities for subsalt imaging: SEG Technical Program Expanded Abstracts.

Sirgue, L., O.I.Barkved, J. V. Gestel, O. Askim, and R. Kommedal, 2009, 3D waveform inversion on Valhall wide-azimuth OBC: EAGE 71th Conference.

Tarantola, A., 1984, Inversion of seismic reflection data in the acoustic approximation: Geophysics, **49**, 1259–1266.

Vigh, D. and E. W. Starr, 2008, 3d prestack plane-wave, full-waveform inversion: Geophysics, **73**, 135–144.

Virieux, J. and S. Operto, 2009, An overview of full-waveform inversion in exploration geophysics: Geophysics, **74**, WCC1–WCC26.

Zhang, S., G. Schuster, and Y. Luo, 2011, Wave-equation reflection traveltime inversion: SEG Technical Program Expanded Abstracts.